

**Classical statistical model for distributions of escape events in swept-bias Josephson junctions**

James A. Blackburn

*Physics and Computer Science, Wilfrid Laurier University, Waterloo, Ontario, Canada*

Matteo Cirillo

*Dipartimento di Fisica and MINAS-Laboratory, Università di Roma "Tor Vergata," I-00133 Roma, Italy*

Niels Grønbech-Jensen

*Department of Applied Science, University of California, Davis, California 95616, USA, and**Niels Bohr International Academy, Niels Bohr Institute, Blegdamsvej 17, DK-2100 Copenhagen, Denmark*

(Received 24 August 2011; revised manuscript received 8 February 2012; published 5 March 2012)

We have developed a model for experiments in which the bias current applied to a Josephson junction is slowly increased from zero until the junction switches from its superconducting zero-voltage state and the bias value at which this occurs is recorded. Repetition of such measurements yields experimentally determined probability distributions for the bias current at the moment of escape. Our model provides an explanation for available data on the temperature dependence of these escape peaks. When applied microwaves are included, we observe an additional peak in the escape distributions and demonstrate that this peak matches experimental observations. The results suggest that experimentally observed switching distributions, with and without applied microwaves, can be understood within classical mechanics and may not exhibit phenomena that demand an exclusively quantum mechanical interpretation.

DOI: [10.1103/PhysRevB.85.104501](https://doi.org/10.1103/PhysRevB.85.104501)

PACS number(s): 74.50.+r, 85.25.Cp, 03.67.Lx

**I. INTRODUCTION**

In 1974, Fulton and Dunkleberger<sup>1</sup> demonstrated the way in which a biased Josephson junction could be thermally excited from its zero-voltage state. More precisely, they conducted experiments in which the bias current was steadily increased from zero to its critical current. In the absence of any noise, thermal or otherwise, the junction would not switch until the bias current reached the critical value. However, with thermal noise, junctions were observed to switch with high probability at bias currents that were slightly less than the critical value. This type of experiment has proven to be an extremely useful tool for probing the details of effective models of the junctions themselves. Later work by Voss and Webb<sup>2</sup> extended the experiments to much lower temperatures, and they found what was interpreted to be evidence that the junction had entered a mode where an escape might be treated as Macroscopic Quantum Tunneling (MQT) out of the effective potential well associated with junction phase dynamics.

Once the idea of macroscopic quantum behavior for Josephson junctions at low temperatures became accepted, the possibility of the manifestation of discrete quantum levels within the effective potential wells received attention. The first experiment to consider this proposition was reported by Martinis, Devoret, and Clarke (MDC).<sup>3</sup> In that experiment, microwaves were directed onto a junction and the bias current was swept as before. The idea was that the microwaves would excite transitions from a lower to a higher level within the well and that the macroscopic quantum variable—the junction phase—would then tunnel out of the well from that higher level, resulting in an escape from the zero-voltage state. Single and multiple peaks in the escape distributions of two samples were reported in their experiment. These data were interpreted as signatures of the anticipated level transitions dictated by quantum theory.

Previously we analyzed the issue of the classical resonant frequencies in wells under both harmonic and anharmonic approximations and found<sup>4</sup> that the classical theory gave results in good agreement with the experiments of MDC, suggesting that the classical Resistive and Capacitive Shunted Junction (RCSJ) model for a Josephson junction might have been dismissed prematurely in favor of the macroscopic quantum picture.<sup>5</sup> The importance of the anharmonic component to the potential well is evident from the fact that a measurement of escape cannot be realized in a harmonic well and, thus, one should not expect meaningful agreement between switching experiments and classical analysis of plasma oscillations. This notion was first presented in Ref. 6, in which the anharmonic theory successfully compared to accompanying experiments on both direct and harmonic resonant switching. It should be mentioned that the anharmonic classical RCSJ approach has since produced good agreement with other experimentally observed features, such as Rabi oscillations and Ramsey fringes,<sup>7,8</sup> as well as tomographic reconstruction of anticipated density matrices for a pair of capacitively coupled Josephson junctions,<sup>9</sup> which originally had been interpreted exclusively in terms of quantum entanglement.

While the nonquantized RCSJ model has been proven to replicate the primary resonant features of the experiments, available experimental reports on switching during bias sweep contain details not yet directly analyzed using the nonquantized approach. One is the saturation of the width of the switching distribution as the thermodynamic temperature is lowered, interpreted as a signature of a quantum crossover temperature;<sup>2</sup> another is the set of multiple resonant switching peaks, interpreted as signatures of quantized energy transitions in the potential well.<sup>3</sup>

In this paper, we reconsider the evidence for the macroscopic quantum tunneling interpretation of these experiments.

In particular, in the spirit of Kramers's statistical analysis,<sup>10</sup> we develop a simple model of the swept-bias type of experiment based on classical thermal activation and show that it gives an excellent accounting of the peaks observed in a number of key experiments.

## II. MODELING A JOSEPHSON SWEEP-BIAS EXPERIMENT

We consider Josephson junctions to be characterized by a supercurrent  $I_C \sin \varphi$  with critical current  $I_C$  junction phase  $\varphi$ , and a capacitance  $C$ . The associated junction plasma frequency is  $\omega_J = \sqrt{2\pi I_C / \Phi_0 C}$ , where  $\Phi_0 = h/2e$  is the flux quantum. We assume junctions whose physical dimensions are much smaller than the Josephson penetration depth.

From this perspective, the phase dynamics of a single Josephson junction subjected to a dc bias is equivalent to the motion of a particle on a washboard potential.<sup>11</sup> The particle sits in a potential well, which becomes shallower at high bias currents. This in turn leads to an enhanced probability of noise-activated escape. If the bias current is swept from 0 toward  $I_C$ , then at some moment the junction will be observed to escape from its potential well and switch to a running state with finite voltage. In the experiments to which we refer, this process was repeated many times in order to acquire a statistical profile of the distribution of bias currents for which the escapes from the zero-voltage state occur.

For our numerical simulations, we imagine an equivalent scenario. Suppose there is an ensemble of  $M$  Josephson junctions. The bias on all junctions starts at 0 and is incremented in  $N$  steps, with each step of duration  $\Delta t = (Nf_S)^{-1}$ , where  $f_S$  is the sweep frequency. Each step is assigned a channel, and the total counts in that channel indicate how many junctions have switched to a finite-voltage state (escape from the potential well) during that interval. As the bias sweep proceeds, the original ensemble will have lost  $e_1$  junctions in the first interval,  $e_2$  junctions in the second interval, and so forth. Consequently, at the beginning of the  $n$ th bias interval, there will be  $M - \sum_{j=1}^{n-1} e_j$  junctions not yet escaped. The number from this remaining pool of junctions that will escape during the next  $\Delta t$  seconds will be

$$e_n = \left[ M - \sum_{j=1}^{n-1} e_j \right] \Gamma(t_n) \Delta t, \quad n = 2, 3, \dots, N, \quad (1)$$

where  $\Gamma(t_n)$  is the probability of escape per unit time in the  $n$ th interval. Of course, the initial interval just satisfies

$$e_1 = M \Gamma(t_1) \Delta t. \quad (2)$$

Equations (1) and (2) will mimic a swept-bias experiment provided a suitable expression is available for the escape rate  $\Gamma$ .

In Kramers's theory,<sup>10</sup> the thermal escape rate can be expressed as

$$\Gamma(t_n) = f_n \exp\left(-\frac{\Delta U_n}{k_B T}\right), \quad (3)$$

where  $f_n$  is the plasma frequency for the well specific to the  $n$ th bias interval and  $\Delta U_n/k_B T$  is the height of the potential

barrier divided by the mean thermal energy. Voss and Webb<sup>2</sup> assumed an escape rate in this form.

However, there has been an ongoing discussion regarding the suitability of the Kramers expression, and as Devoret *et al.*<sup>12</sup> and others have pointed out, a better equation for the escape rate, from Büttiker, Harris, and Landauer (BHL),<sup>13</sup> is

$$\Gamma_{BHL}(t_n) = a_t f_n \exp\left(-\frac{\Delta U_n}{kT}\right), \quad (4)$$

where

$$a_t = \frac{4\alpha}{\left[1 + \sqrt{\left(1 + \frac{\alpha Q k_B T}{1.8 \Delta U_n}\right)}\right]^2}. \quad (5)$$

According to Devoret *et al.*,<sup>12</sup>  $\alpha = 1.4738$ . In this expression,  $Q$  is a parameter that quantifies the dissipation in the junction; low dissipation corresponds to large  $Q$ . Devoret *et al.*<sup>14</sup> noted that “the prefactor depends only weakly on  $Q$ ” and they consequently used an escape rate in the form of Eq. (3). Similarly, Devoret *et al.* in Ref. 12 stated that the value of the prefactor  $a_t$  is “close to unity.”

For these reasons, we proceed with our classical simulations of swept-bias experiments using expression (3) for the escape rate. We consider the second-order effects of  $Q$  in Sec. VI.

In the harmonic approximation

$$f_n = f_J \sqrt{1 - \eta_n^2}, \quad (6)$$

with  $\eta_n$  being the normalized bias current within the  $n$ th bias interval.

Combining these expressions, we obtain

$$\Gamma(t_n) \Delta t = \left[ \left( \frac{f_J}{N f_S} \right) \sqrt{1 - \eta_n^2} \right] \exp\left(-\frac{\Delta U_n}{k_B T}\right), \quad (7)$$

which is required in Eq. (1). The prefactor before the exponential represents the number of plasma oscillations that can fit within the time window of the  $n$ th data acquisition channel—that is, the number of attempts that will occur in that time window.

According to MQT theory, at sufficiently low temperatures tunneling of the phase variable becomes the dominant escape mechanism, in which case the escape rate takes the form

$$\Gamma_q = a_q f_n \exp\left[-7.2 \frac{\Delta U_n}{h f_n} \left(1 + \frac{0.87}{Q} + \dots\right)\right], \quad (8)$$

where

$$a_q = \left[ 120\pi \left( \frac{7.2 \Delta U_n}{h f_n} \right) \right]^{\frac{1}{2}}. \quad (9)$$

Clearly, in contrast to the classical expression Eq. (3), this escape rate does not depend on temperature. Voss and Webb<sup>2</sup> pointed out that the transition from classical to quantum behavior should take place around a “crossover temperature” satisfying

$$T_{cr} \approx \frac{h f}{7 k_B}. \quad (10)$$

### III. MICROWAVES OFF

The height of the barrier at the  $n$ th step is given by the well-known expression

$$\Delta U_n = 2 \frac{I_C \Phi_0}{2\pi} \left[ \sqrt{1 - \eta_n^2} - \eta_n \cos^{-1} \eta_n \right], \quad (11)$$

so

$$\frac{\Delta U_n}{k_B T} = \frac{2}{\beta} \left[ \sqrt{1 - \eta_n^2} - \eta_n \cos^{-1} \eta_n \right], \quad (12)$$

where

$$\beta = \left( \frac{2\pi k_B}{\Phi_0} \right) \frac{T}{I_C}. \quad (13)$$

#### A. Voss and Webb (1981)

As an example of an experimental simulation, parameters were chosen to be  $N = 5000$ ,  $M = 100\,000$ ,  $f_J = 35.53$  GHz, and  $f_S = 10$  Hz, numbers consistent with the experiments of Voss and Webb<sup>2</sup> (although they gave no value for the number of channels in their system). The evolution of the peaks shown in Fig. 1 is in very good agreement with the experimental data in Fig. 1 of Voss and Webb.<sup>2</sup> Also shown in Fig. 1 is the single MQT peak from a simulation using the escape rate expression Eq. (8) with  $Q = 50$ . The conclusion to be drawn is that when the value of  $\beta$  drops below a crossover equivalent, macroscopic quantum behavior should take over from the classical escape process and the temperature-independent peak marked MQT should become frozen in place. In such a case not only the peak widths but also the peak positions must remain constant. Then, none of the classical peaks to the right of MQT would be observed in an experiment.

The crossover temperature, Eq. (10), is a function of the natural frequency of a particular well, and this in turn is controlled by the applied bias current as specified in Eq. (6). Therefore, in a swept-bias experiment, one is also sweeping the natural frequency of the continuously varying well shape.

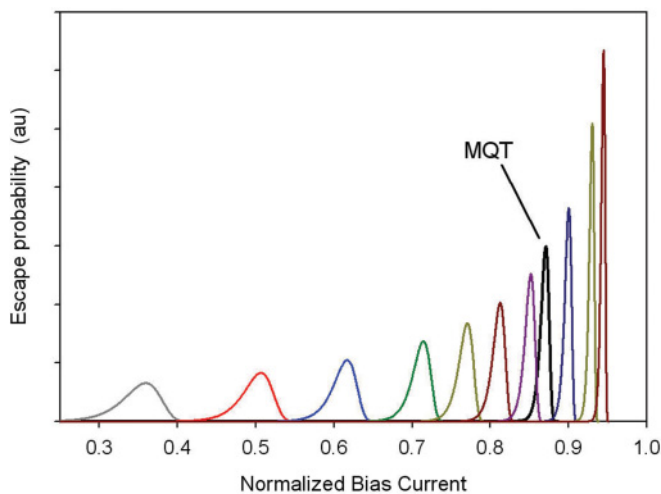


FIG. 1. (Color online) Simulation results for a swept-bias experiment. The ten classical peaks had  $\beta$  values (left to right) of 0.0551, 0.0375, 0.0259, 0.0169, 0.0123, 0.0092, 0.00656, 0.00372, 0.00223, 0.00160. The single escape peak labeled MQT was computed using expression (8) for the escape rate with  $Q = 50$ .

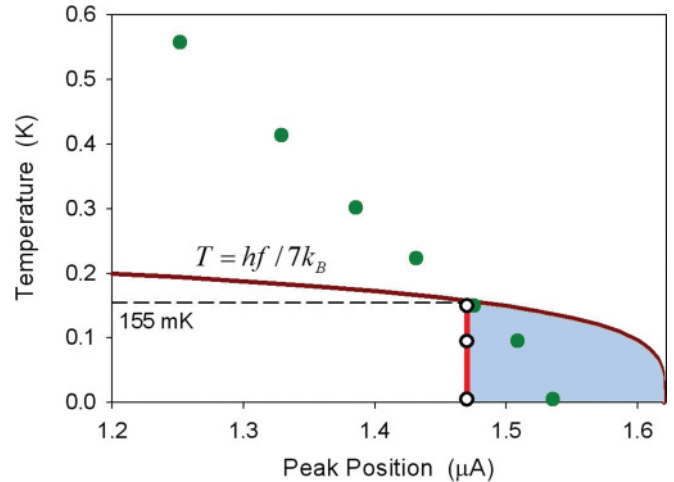


FIG. 2. (Color online) Dependence of the crossover temperature on bias current, for sample parameters of Voss and Webb.<sup>2</sup> Dots mark the positions of the seven lowest temperature peaks shown in Fig. 1 of Ref. 2. At  $1.470 \mu\text{A}$ , the experimental data drop below the crossover boundary. According to the MQT hypothesis, the escape peaks should then become temperature independent and peak positions would be expected to lie on the vertical line, as depicted by open circles.

It is simple to use Eqs. (6) and (10) to plot the dependence of crossover temperature on bias current; this is shown in Fig. 2. The positions (bias values) of the experimental peaks, indicated by solid dots, were manually extracted from Fig. 1 in Ref. 2 using digitizing software.<sup>15</sup> A vertical line marks the point at which the sample temperature has dropped below the crossover characteristic; this occurs at  $T \approx 155$  mK and a bias of  $1.470 \mu\text{A}$ . Note that the two experimental escape peaks for temperatures  $T = 95$  mK and  $T = 5$  mK are below the anticipated quantum transition temperature and appear not to have frozen at  $1.470 \mu\text{A}$ , but instead continue to advance beyond the MQT stopping point into the shaded “forbidden” zone. While this progression of escape peaks toward higher bias values is contrary to the expectations of the MQT model, it is consistent with the classical escape model.

The apparent saturation of the widths of the escape peaks below the crossover temperature, noted in Ref. 2 was claimed to constitute the “first compelling evidence for the existence of quantum tunneling of a macroscopic variable.” Using digitizing software, the experimental data points for the peak widths were extracted from Fig. 3 in Ref. 2. These points are plotted in Fig. 3. More than twenty years ago, Cristiano and Silvestrini<sup>16</sup> proposed that the presence of some additional noise could raise the sample temperature above the bath temperature  $T$  such that  $T_{\text{eff}} = T + T_N$ . In particular, they demonstrated that the observed temperature dependence of the peak widths in Ref. 2 could be replicated using  $T_N = 63$  mK and with classical escape theory alone. Such an elevated sample temperature, possibly due to self-heating, was also noted in Ref. 17.

We have run our simulation with  $T$  replaced by  $T_{\text{eff}}$  and  $T_N = 63$  mK, and the results, virtually identical to those in Ref. 16, are shown in Fig. 3. By most standards, the agreement between experiment and classical theory is excellent. A vote in favor of a quantum signature in these data could only be

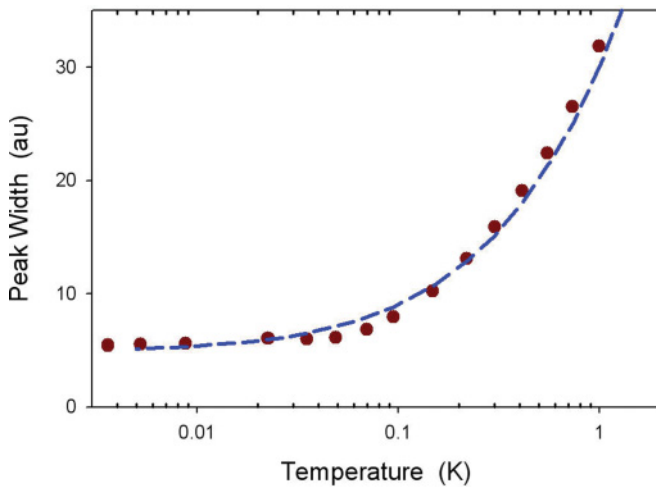


FIG. 3. (Color online) Dots: experimental peak widths from Fig. 3 of Ref. 2. Dashed line: classical simulation with an effective sample temperature of  $T + 63$  mK, where  $T$  is the bath temperature.

supported by a much finer analysis including error bars in the experimental peak widths. As it stands, the classical model fits the experimental data exceptionally well over two orders of magnitude in bath temperature with the above-mentioned suggested effective sample temperature.

#### IV. MICROWAVES ON

We now consider appropriate modifications to the swept-bias model needed to take into account the action of applied microwaves. In such experiments, a fixed-frequency microwave source is used and the bias current is ramped up.

Our numerical solutions of the equation of motion of the phase<sup>11</sup> with both dc and ac bias reveal induced oscillations around the minimum in the potential well. The amplitude of these oscillations depends on the dc bias chosen. There will be a particular bias,  $\eta_{\text{res}}$ , at which the the oscillation amplitude is a maximum. The question is, what is the value for  $\eta_{\text{res}}$ ?

In the harmonic approximation, the natural frequency of a well is related to the dc bias through Eq. (6). However, as shown in Refs. 4 and 6, when the amplitude of the phase oscillations is large, the cubic nature of the well comes into play and an anharmonic approximation takes the place of Eq. (6):

$$f_n = f_J \sqrt{(J_0(A) + J_2(A)) \sqrt{1 - \left(\frac{\eta_n}{J_0(A)}\right)^2}}, \quad (14)$$

where  $J_p$  is the Bessel function of  $p$ th order, first kind, and  $A$  is the amplitude of the oscillation. Thus, the resonance frequency is depressed for increasing oscillation amplitudes  $A$ . It has been found that situations in which resonant states produce nonzero and nonunity switching probabilities are given for oscillation amplitudes near the inflection point of the potential well. In the limit  $\eta \rightarrow 1$ , this value of  $A$  is given by the explicit expression  $A^2 \approx \frac{4}{3}(1 - \eta_{\text{res}})$ .

Setting  $f_n = f_{ac}$  in Eq. (6) would give one answer for the resonant bias  $\eta_{\text{res}}$ , while Eq. (14) would give a slightly smaller answer. This means that without knowledge of the strength of the microwaves at the junction, the best one can say is that  $\eta_{\text{res}}$

must lie somewhere below the value for  $A = 0$  (as also seen experimentally in Ref. 18) and in the vicinity of the interval spanned by the two values for  $A = 0$  and  $A^2 \approx \frac{4}{3}(1 - \eta_{\text{res}})$ . As an example, for a microwave frequency  $f_{ac}/f_J = 0.350$ , the limits of  $\eta_{\text{res}}$  are 0.9925 and 0.9887.

Let the amplitude of the induced phase oscillation to the right of the minimum point of any well be denoted  $\delta\varphi_n$ . For not too large excitations,  $\delta\varphi$  has a bell-shaped distribution, centered at  $\eta_{\text{res}}$ . At  $\eta_{\text{res}}$  the ac field is transferring a maximum amount of energy into the junction. On either side of this optimum bias, the amplitude of the phase oscillations diminishes and the absorbed energy declines. For a bell-shaped distribution of  $\delta\varphi$  we used the following heuristic expression:

$$\delta\varphi_n = a \frac{b^2}{(\eta_n - \eta_{\text{res}})^2 + b^2}. \quad (15)$$

There are two parameters here:  $b$ , which sets the sharpness of the distribution, and  $a$ , which sets the peak value.

Whenever sustained phase oscillations are induced, the added energy is

$$\frac{\Delta U_{1n}}{k_B T} = \beta^{-1} \{ [-\cos \varphi_{\text{max}} - \eta_n \varphi_{\text{max}}] - [-\cos \varphi_{\text{min}} - \eta_n (\varphi_{\text{min}})] \} \quad (16)$$

with  $\varphi_{\text{min}} = \sin^{-1} \eta_n$  and  $\varphi_{\text{max}} = \varphi_{\text{min}} + \delta\varphi_n$ . This will reduce the escape barrier in the  $n$ th interval to an effective value

$$\frac{\Delta U_{\text{eff}}}{k_B T} = \frac{\Delta U_n}{k_B T} - \frac{\Delta U_{1n}}{k_B T}, \quad (17)$$

and this is what thermal noise needs to overcome. This effective barrier height replaces the original in Eq. (7) and then the simulation can proceed as before.

We now apply this simulation to several sets of published data. First we consider experiments which showed only a single microwave-induced escape peak.

##### A. Single microwave-induced peaks

As already noted, swept-bias experiments yield histograms for the escape probability. Some authors prefer to convert such data to escape rates  $\Gamma$  as a function of bias current. Then a *relative rate*, with and without microwaves,  $[\Gamma(P) - \Gamma(0)]/\Gamma(0)$ , may be plotted. This has the effect of stripping away the thermal escape peak (as discussed in Secs. III and IV), thereby isolating purely microwave-induced phenomena.

###### 1. Martinis *et al.* (1985)

Consider the results presented in Martinis *et al.*<sup>3</sup> Their Fig. 3 is reproduced in the upper panel of Fig. 4. The junction was characterized by the following parameter values:  $I_C = 9.489 \mu\text{A}$  and  $C = 6.35 \text{ pF}$ . This gives a junction zero-bias plasma frequency  $f_J = 10.72 \text{ GHz}$ ; hence the microwave frequencies of 3.7, 3.6, 3.5, and 3.4 GHz correspond to 0.3451, 0.3358, 0.3265, and 0.3172 in dimensionless form. This experiment was carried out at  $T = 18 \text{ mK}$ .

For comparisons of these experiments with classical results, we simply make use of the escape rate expression, Eq. (3), with a barrier given by Eq. (12) in the absence of microwaves or with a reduced effective barrier given by Eq. (17) when



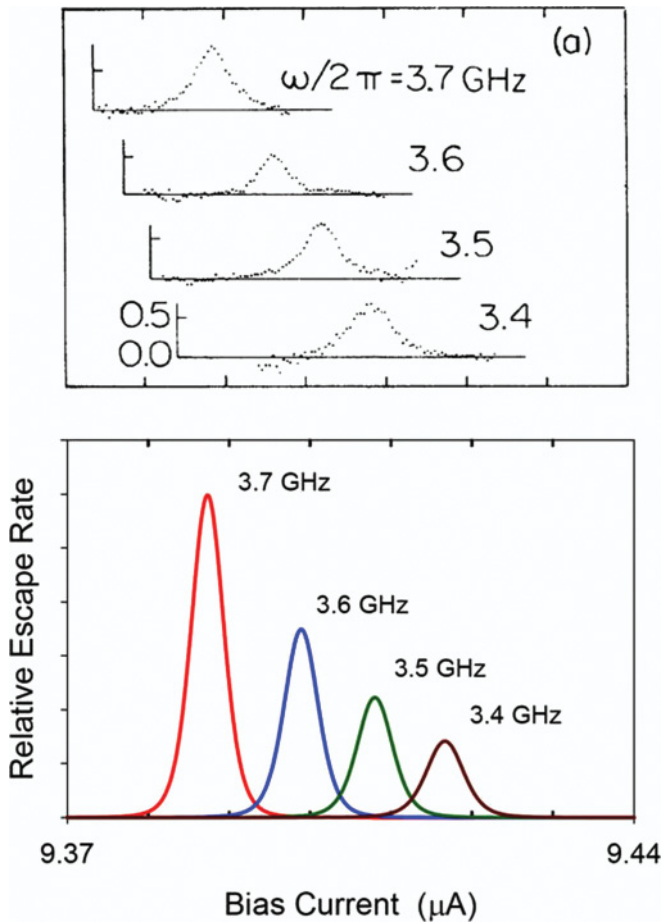


FIG. 4. (Color online) Comparison of the experimental results of Martinis *et al.*<sup>3</sup> (top) with our simulation (bottom).

microwaves are present. For each of the four microwave frequencies, the anharmonic result, Eq. (14), was used to obtain the bias current  $\eta_{\text{res}}$  which selects the well that is resonant with the excitation. With this normalized bias, Eq. (16) together with Eq. (15) permits the reduced barrier height to be calculated.

The remainder of the parameters chosen to match the situation were  $a = 0.10$ ,  $b = 0.0010$ , and  $\beta = 0.0000796$ . The results for the classical escape-rate calculations are shown in the lower panel of Fig. 4. As can be seen, the classical results agree very well with the experimentally observed peaks in the escape rates for these four microwave frequencies.

### 2. *Thraikill et al. (2009)*

Thraikill *et al.*<sup>19</sup> carried out swept-bias experiments on a Josephson junction characterized by  $I_C = 9.485 \mu\text{A}$  and  $C = 4.7 \text{ pF}$ . The Josephson plasma frequency was thus  $f_J = 12.46 \text{ GHz}$ . The escape probability distributions were measured at several different combinations of temperature and microwave frequency, as shown in the upper panel of Fig. 5. For the classical simulations, the parameter values were  $a = 0.09$ ,  $b = 0.003$  (equivalent to a half-width in the distribution of  $0.028 \mu\text{A}$ ) and from top to bottom,  $\eta_{\text{res}} = 0.972$ ,  $0.976$ ,  $0.980$ , and  $0.984$ . The simulation results clearly are in very good agreement with the experimental data. Note that

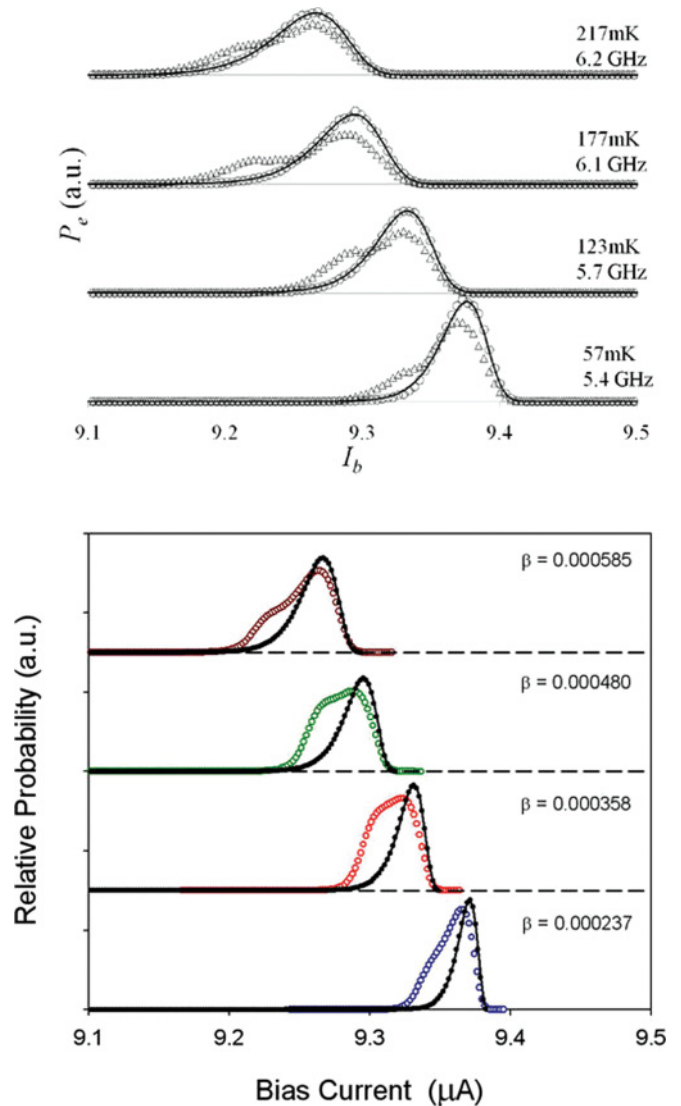


FIG. 5. (Color online) Comparison of experimental data from Thraikill *et al.*<sup>19</sup> (top) and our simulation results (bottom). where closed circles indicate results without microwaves.

the ac resonance and the thermal peak are nearly on top of each other, so the peaks almost merge. Also, the simulation exhibits the same shifting effect as in the experiments: The thermal peak without microwaves becomes displaced slightly toward lower bias values when the microwaves are turned on.

### B. Multiple microwave-induced peaks

Every swept-bias experiment with microwaves present yields at least one ac induced escape peak. This includes both Figs. 2 and 3 in Ref. 3, Fig. 3 in Ref. 17, Fig. 2 in Ref. 19, and Fig. 6.5 in Ref. 20, but only in two instances was a second microwave peak in evidence.

In Fig. 2, of Ref. 3, one of the experimental samples exhibited an additional microwave escape peak. For that experiment, the sample parameters were  $I_C = 30.572 \mu\text{A}$ ,  $C = 47 \text{ pF}$ , and so  $f_J = 7.07 \text{ GHz}$ . Hence the normalized microwave frequency of  $2 \text{ GHz}$  was  $0.2829$ . The two peaks

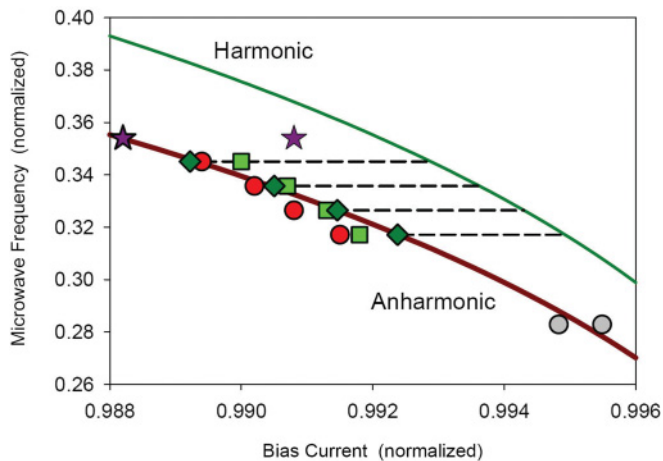


FIG. 6. (Color online) Comparison of classical model and quantum model with experimental data. Circles are experimental points, squares are predictions of the quantum model [digitized from the positions of the arrow markers in Fig. 3(b) in Ref. 3], and diamonds are predictions of the classical model using the anharmonic approximation for resonance frequencies in Eq. (14). The harmonic approximation, Eq. (6), is also plotted. The bottom pair of points are taken from the experimental data in Fig. 2 of Ref. 3; the upper pair of points (stars) are the two observed peaks from Fig. 3 in Ref. 17.

were at  $30.43424 \mu\text{A}$  and  $30.41391 \mu\text{A}$ , which in normalized units are 0.995490 and 0.994829. These two points are included in Fig. 6; they are both quite close to the anharmonic curve.

In Fig. 3 of Ref. 17, there are two microwave-induced escape peaks. The sample parameters were  $I_C = 14.12 \mu\text{A}$ ,  $C = 4.2 \text{ pF}$ , yielding a junction plasma frequency  $f_J = 16.1 \text{ GHz}$ . The microwave frequency was  $5.7 \text{ GHz}$ , which is 0.354 in normalized units. The two peaks are at bias currents of  $I = 13.9907 \mu\text{A}$  and  $I = 13.9530 \mu\text{A}$ , which in normalized units are 0.9908 and 0.9882. These two points are included in Fig. 6. Interestingly, one appears to be on the anharmonic curve, while the other is close to the harmonic curve, perhaps suggesting that the system can resonantly respond to either condition. The possibility for multiple states in the ac-driven anharmonic potential is consistent with previously reported observations (see Fig. 1 in Ref. 8). It should be pointed out that the solid line in Berkley’s Fig. 3 was described as “a Lorentzian fit to two peaks,” meaning it is not in any sense a theoretical prediction and so does not constitute confirmation of quantum expectations. The labeling of the two peaks as  $|1\rangle \rightarrow |2\rangle$  and  $|0\rangle \rightarrow |1\rangle$  is based on assumptions regarding applicable physics.

In the previous section, it was noted that the four single peaks, each at a different microwave frequency, from Fig. 3 of Ref. 3 are reasonably reproduced by classical calculations of relative escape rates. These classical points are shown in Fig. 6 as diamonds that lie along the anharmonic curve. However, the comparison of experiments with classical and quantum theories described in Ref. 3 contained the following statement: “Furthermore, the measured positions of the resonances are clearly very different from a classical prediction for the resonant activation of the particle oscillating at the plasma frequency (dashed line).” This dashed line appears in part (b)

of the figure and is in fact the harmonic approximation, but we see from our Fig. 6 that the fair test of the classical model is the anharmonic approximation, and at the very least the classical model is as successful as the quantum hypothesis.

## V. EFFECT OF SWEEP FREQUENCY

It is important to note that peaks in the escape probability distributions are not like lines in atomic spectra in that they are a manifestation of both the fundamental physics associated with escape rates and the way the experiment is performed—specifically, the frequency at which the bias current is swept from zero to its critical value, ( $f_S$ ). This issue was addressed in a swept-bias simulation with:  $N = 50,000$ ,  $M = 100,000$ ,  $f_J = 7.072 \text{ GHz}$ ,  $f_S = 10 \text{ Hz}$ , and  $\beta = 0.00129$ . The results for microwaves off are shown in Fig. 7. Clearly, the exact location and shape of the thermal escape peak are determined in part by the speed with which the bias current is ramped toward the critical value. As might be anticipated, increasing the sweep rate moves the peak toward higher bias currents.

## VI. EFFECT OF DISSIPATION

To illuminate some aspects of the effects of dissipation, we carried out swept-bias simulations using Eqs. (4) and (5), and for this example with parameters  $I_C = 14.12 \mu\text{A}$ ,  $C = 4.2 \text{ pF}$ , and  $\beta = 0.00018$ . The microwave frequency was set at  $5.7 \text{ GHz}$  and the assumed excitation parameters were  $a = 0.085$  and  $b = 0.0012$ . Typical values of the dissipation  $Q$  for underdamped Josephson junctions lie in the range 20 to 50. Escape histograms were repeated for a number of choices of the dissipation constant parameter, and the results are shown in Fig. 8. Note that the microwave peak does not shift, but the position of the purely thermal peak varies with  $Q$ . Therefore, the particular value of the junction dissipation might have a slight effect on predictions of the Voss and Webb-type of experiment but would not influence the positions of microwave-induced peaks.

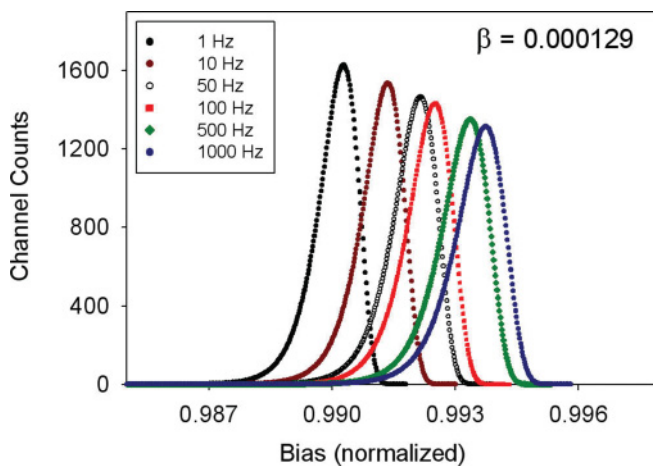


FIG. 7. (Color online) Simulation results showing the effects of bias sweep frequency  $f_S$  on the position of the peak in the escape probability distribution.

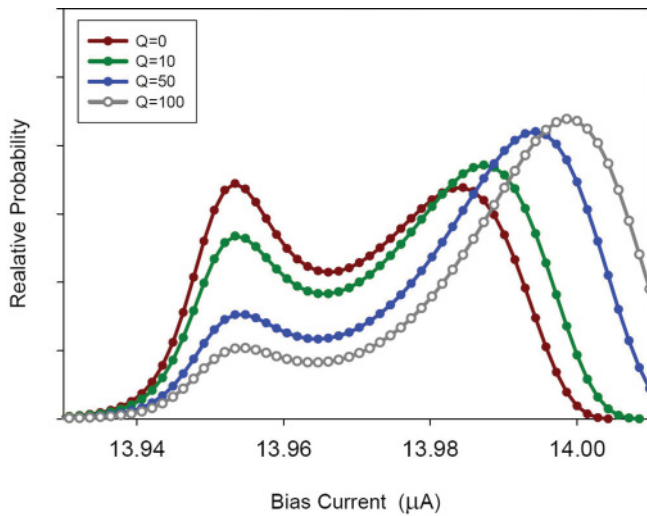


FIG. 8. (Color online) Swept bias simulations with selected values of the parameter  $Q$  using the escape rate due to Büttiker, Harris, and Landauer.<sup>13</sup>

## VII. DISCUSSION

The decades-old papers of Voss and Webb and Martinis *et al.* appeared to convincingly demonstrate the (anticipated) appearance of MQT in superconducting circuits operating below a crossover temperature. The classical model was subsequently discarded as a possible source for observed phenomena at millikelvin temperatures. In this paper we

have shown that this assertion may not be justified, and that these early foundational experiments can certainly be modeled successfully within a purely classical device description.

With respect to the experiments of Voss and Webb, we have demonstrated that there was not strong evidence that the junction had entered a macroscopic quantum state even at the lowest temperatures. A classical model with some self-heating gives a more consistent description of those observations.

With respect to the experiments of Martinis *et al.*, we have demonstrated that in the presence of microwave irradiation the additional peaks which appear in the swept-bias escape distributions are just as well accounted for within the classical resonant activation model as by the proposed macroscopic quantum model.

The key issue in this situation was nicely expressed by Devoret *et al.*<sup>21</sup> as follows: “An experiment cannot prove a theory, but only invalidate an alternative theory.” The present study should therefore be seen in this context—the classical theory for these systems has not yet been ruled out. Therefore, an exclusive presumption of MQT in these systems is not justified.

## ACKNOWLEDGMENTS

We thank R. C. Ramos for providing the copy of his experimental data included in Fig. 5. This work was supported (J.A.B.) by a grant from the Natural Sciences and Engineering Research Council of Canada, and (M.C.) by the MIUR-PRIN08 program (Italy). N.G.J. is grateful for support from Danmarks Nationalbank (Denmark).

<sup>1</sup>T. A. Fulton and L. N. Dunkleberger, *Phys. Rev. B* **9**, 4760 (1974).

<sup>2</sup>R. F. Voss and R. A. Webb, *Phys. Rev. Lett.* **47**, 265 (1981).

<sup>3</sup>J. M. Martinis, M. H. Devoret, and J. Clarke, *Phys. Rev. Lett.* **55**, 1543 (1985).

<sup>4</sup>J. A. Blackburn, M. Cirillo, and N. Grønbech-Jensen, *Phys. Lett. A* **374**, 2827 (2010).

<sup>5</sup>A. J. Leggett, *Jpn. J. Appl. Phys.* **26**, 1986 (1987), Supplement 26-3.

<sup>6</sup>N. Grønbech-Jensen and M. Cirillo, *Phys. Rev. B* **70**, 214507 (2004); N. Grønbech-Jensen, M. G. Castellano, F. Chiarello, M. Cirillo, C. Cosmelli, V. Merlo, R. Russo, and G. Torrioli, in *Quantum Computing: Solid State System*, edited by B. Ruggeiro, P. Delsing, C. Granta, Y. Paskin, and P. Silvestrini (Kluwer, New York, 2006), pp. 111–119.

<sup>7</sup>J. E. Marchese, M. Cirillo, and N. Grønbech-Jensen, *Phys. Rev. B* **79**, 094517 (2009).

<sup>8</sup>N. Grønbech-Jensen and M. Cirillo, *Phys. Rev. Lett.* **95**, 067001 (2005).

<sup>9</sup>J. A. Blackburn, J. E. Marchese, M. Cirillo, and N. Grønbech-Jensen, *Phys. Rev. B* **79**, 054516 (2009); N. Grønbech-Jensen, J. E. Marchese, M. Cirillo, and J. A. Blackburn, *Phys. Rev. Lett.* **105**, 010501 (2010).

<sup>10</sup>H. A. Kramers, *Physica (Amsterdam)* **7**, 284 (1940).

<sup>11</sup>T. van Duzer and C. W. Turner, *Principles of Superconductive Devices and Circuits*, 2nd ed. (Prentice Hall, Englewood Cliffs, NJ, 1999), Chap. 5.

<sup>12</sup>M. H. Devoret, D. Esteve, J. M. Martinis, A. Cleland, and J. Clarke, *Phys. Rev. B* **36**, 58 (1987).

<sup>13</sup>M. Büttiker, E. P. Harris, and R. Landauer, *Phys. Rev. B* **28**, 1268 (1983).

<sup>14</sup>M. H. Devoret, J. M. Martinis, D. Esteve, and J. Clarke, *Phys. Rev. Lett.* **53**, 1260 (1984).

<sup>15</sup>The software is GRAB IT! from Datatrend Software, Raleigh, NC.

<sup>16</sup>R. Cristiano and P. Silvestrini, *Il Nuovo Cimento, Note Brevi* **10**, 869 (1988).

<sup>17</sup>A. J. Berkley, H. Xu, M. A. Gubrud, R. C. Ramos, J. R. Anderson, C. J. Lobb, and F. C. Wellstood, *Phys. Rev. B* **68**, 060502 (2003); on page 3 of this paper is this comment: “The 60 mK temperature was 40 mK above the base temperature, probably due to self-heating.”

<sup>18</sup>N. Grønbech-Jensen, M. G. Castellano, F. Chiarello, M. Cirillo, C. Cosmelli, L. V. Filippenko, R. Russo, and G. Torrioli, *Phys. Rev. Lett.* **93**, 107002 (2004).

<sup>19</sup>Z. E. Thraillkill, J. G. Lambert, S. A. Carabello, and R. C. Ramos (unpublished); R. C. Ramos (private communication).

<sup>20</sup>S. K. Dutta, Ph.D. thesis, University of Maryland, 2006; note that other multipeak escape histograms appearing in this thesis are relative to interferometers and not to single junctions.

<sup>21</sup>M. H. Devoret, J. M. Martinis, and J. Clarke, *Phys. Rev. Lett.* **63**, 212 (1989).